

Thermally Activated Magnetization Rotation in Small Nanoparticles

Vassilios Tsiantos, *Member, IEEE*, Thomas Schrefl, *Member, IEEE*, Werner Scholz, Hermann Forster, Dieter Suess, Rok Dittrich, and Josef Fidler, *Member, IEEE*

Abstract—In this paper, we test the performance and validity of a semi-implicit time-integration scheme, originally applied in quantum dynamics, for use in micromagnetics. The attempt frequency and energy barriers are calculated for Co nanoparticles. Moreover, a fit of the relaxation time to the Arrhenius–Neel law is presented. The semi-implicit time-integration method is very robust and allows time steps up to 3 ps at a temperature of 50 K.

Index Terms—Magnetic reversal, thermal activation, thermal stability, thermal switching.

I. INTRODUCTION

WITH DECREASING device dimensions, thermal fluctuations may ultimately limit the performance of magnetic materials used for spin valve sensors [1], magnetic random access memory (MRAM) cells [2], or magnetic storage media [3]. Thermal effects were included in micromagnetic simulations. The computer models either solve the stochastic Landau–Lifshitz–Gilbert (LLG) equation (Langevin) [4], where a random fluctuating field mimics the thermal excitations, or apply the Monte Carlo method on an assembly of Heisenberg spins [5].

Langevin micromagnetics treats finite temperature effects by adding a thermal fluctuation field to the effective field [6]. Uniform rotation of the magnetization is expected for small single particles. However, a comparison of theory with experiment is difficult, because often a nonuniform magnetization is observed, due to complicated shapes and surfaces, crystalline defects, and surface anisotropy [7].

In this paper, the attempt frequency and energy barriers are calculated for Co nanoparticles. Furthermore, a fit of the calculated relaxation time to the Arrhenius–Neel law is presented. In addition to this, a curve of the probability of not switching is drawn. A brief discussion of the micromagnetic code is included. Finally, measures of the performance of the simulations are given, such as the number of iterations involved in the algorithm at each time step and the number of calculations of the right-hand side of the Langevin equation.

II. STOCHASTIC LLG EQUATION

The theoretical treatment of thermally activated magnetization reversal for particles with an extension greater than the ex-

change length requires solving the Langevin equation numerically. The Langevin equation follows from the Gilbert equation of motion by adding a random thermal fluctuation field to the effective magnetic field:

$$\frac{\partial \mathbf{J}}{\partial t} = -|\gamma| \mathbf{J} \times (\mathbf{H}_{eff} + \mathbf{H}_{th}) + \frac{\alpha}{J_s} \mathbf{J} \times \frac{\partial \mathbf{J}}{\partial t}. \quad (1)$$

The first term on the right-hand side of (1) accounts for the gyromagnetic precession of the magnetic polarization \mathbf{J} ; the second term arises from viscous damping. After space discretization using the finite-element method, an equation similar to (1) has to be fulfilled at each node of the finite-element mesh [8].

The term γ is the gyromagnetic ratio and α is the Gilbert damping constant. The thermal field is assumed to be a Gaussian random process with the following statistical properties:

$$\langle H_{th,i}^k, H_{th,j}^l \rangle = \varepsilon \delta_{ij} \delta_{kl} \delta(t - t'). \quad (2)$$

The average of the thermal field taken over different realizations vanishes in each direction i in space. The thermal field is uncorrelated in time, uncorrelated at different node points (k, l) of the finite-element mesh, and uncorrelated for different orthogonal vector components ($i \neq j$). The strength of the thermal fluctuations follows from the fluctuation-dissipation theorem [9]:

$$\varepsilon = \frac{2\alpha k_B T}{\gamma J_s V_i} \quad (3)$$

where T is the temperature, V_i is the volume surrounding the node i of the finite-element mesh, and k_B is the Boltzmann constant.

III. TIME-INTEGRATION METHOD

A. Semi-Implicit Algorithm

The main steps of the semi-implicit algorithm are as follows.

- 1) The general form of the semi-implicit scheme is given by [10]

$$\Delta x_{i,j} = A_i(\bar{t}_j, \bar{\mathbf{x}}_j) \Delta t + \sum_n B_{in}(\bar{t}_j, \bar{\mathbf{x}}_j) dW_{n,j} \quad (4)$$

where dW are Gaussian random numbers with mean zero and standard deviation one and B is an $n \times n$ dimensional multiplicative noise term.

- 2) The right-hand side of (4) is evaluated in the middle of the time interval.

Manuscript received January 6, 2003. This work was supported by the Austrian Science Fund under Project Y132-PHY.

The authors are with the Institute of Solid State Physics, Vienna University of Technology, Vienna 1040, Austria (e-mail: v.tsiantos@computer.org; thomas.schrefl@tuwien.ac.at; josef.fidler@tuwien.ac.at).

Digital Object Identifier 10.1109/TMAG.2003.816456

- 3) The midpoint value \bar{x} is obtained by an implicit equation $\bar{x} = (\mathbf{x}_j + \mathbf{x}_{j+1})/2$.
- 4) The equation for the time evolution at the j th time step is now an implicit one, which involves solving for \bar{x} .

The above time-integration scheme treats the deterministic part implicitly, thus, stability problems of explicit integration schemes can be avoided. Time steps up to 4 ps lead to stable solutions.

B. Nonlinear Equation

One way of solving the above-mentioned implicit (nonlinear) equation is by an iterative procedure called *simple iteration*, or *functional iteration*. In our simulations, the functional iteration is stopped when the norm between two successive solution vectors drops below 10^{-10} .

A normal way to measure the efficiency of a code is to solve the problem for a number of different tolerances and plot the cost of the method against the tolerance [11]. The number of function evaluations (NFEs) is a very good approximation of the cost of the micromagnetic simulations. The reason is that in micromagnetic simulations, the evaluation of the function, that is, the evaluation of the Langevin equation, is the most time-consuming part. In a three-dimensional simulation, the function evaluation involves the calculation of exchange and magnetostatic interactions fields. With a convergence criterion of 10^{-10} , the average NFEs per time step is five.

C. MATLAB Implementation

For the implementation of the micromagnetic model, we used MATLAB [12], which is a very powerful tool for micromagnetic simulations of small order. It has the capability of using vectors and matrices in a very efficient way. In our implementation of the semi-implicit scheme, each iteration costs one evaluation of the function f , where f is the right-hand side of the stochastic LLG equation.

The main steps of the code are as follows:

- 1) initialization of the input parameters and constants;
- 2) calculation of ε , (3);
- 3) repeat until end of number of realizations:
 - a) initialization of magnetization;
 - b) repeat until the end time:
 - i) calculation of the deterministic part of the field;
 - ii) brownian increments;
 - iii) calculation of B , the $n \times n$ dimensional multiplicative noise term;
 - iv) calculation of the magnetization at time step $j + 1$;
 - v) normalization.

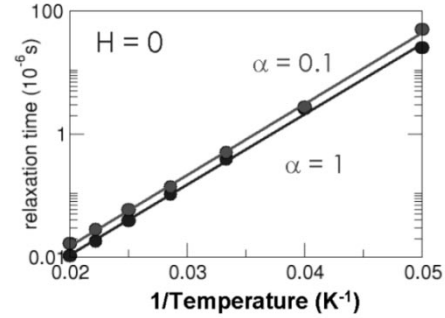


Fig. 1. Relaxation time for the spontaneous rotation of a small Co particle at nonzero temperature and zero applied field.

IV. NUMERICAL EXPERIMENTS

A. Co Nanoparticles

For the experiments, a field lower than the zero temperature switching field applied to a small Co nanoparticle was used. The anisotropy energy used is given by [13]

$$\frac{E_0(\vec{m})}{v} = -K_1 m_z^2 + K_2 m_x^2 - K_4 (m_x^2 m_y^2 + m_x^2 m_z^2 + m_y^2 m_z^2) \quad (5)$$

where K_1 and K_2 are the anisotropy constants along z and x , the easy and hard magnetization axes, respectively. K_4 is the fourth-order anisotropy constant, and the $(x'y'z')$ coordinate system is deduced from (xyz) by a 45° rotation around the z axis. The crystalline anisotropy constants used were $K_1 = 2.2 \times 10^5 \text{ J/m}^3$, $K_2 = 0.9 \times 10^5 \text{ J/m}^3$, and $K_3 = 0.1 \times 10^5 \text{ J/m}^3$, and the saturation polarization J_s was 1.76 T. The particle diameter was 3.18 nm.

First, we performed a numerical telegraph noise experiment. We simulated the thermally induced switching of the particles for different temperatures. From the relaxation time as a function of the inverse temperature, we calculated the attempt frequency ($f_0 = 1.2 \times 10^{10} \text{ Hz}$) and the energy barrier. The energy barrier agrees well with $K_1 V$, as expected for uniform rotation. Fig. 1 shows the fit of the numerical data to the Arrhenius–Neel law for two values of the damping constant α .

Fig. 2 presents the results of numerical waiting time experiments for different applied fields. The external field was varied in the range from $\mu_0 H = 0.186 \text{ T}$ to $\mu_0 H = 0.264 \text{ T}$. The Gilbert damping constant was $\alpha = 0.1$. Again, the energy barriers were derived from a fit to the Arrhenius–Neel law. The energy barrier as a function of the field follows the well-known relation [13]

$$\Delta E = K_1 V \left(1 - \frac{H}{H_0}\right)^2 \quad (6)$$

where H_0 is the intrinsic switching field at $T = 0$.

Fig. 3 gives a histogram of the waiting times at $T = 5 \text{ K}$ and $\mu_0 H = 0.186 \text{ T}$ and the derived probability of not switching. The integral of this histogram (or a cumulative histogram) is proportional to the switching probability $P(t)$, which is the probability that the particle has switched by certain time. The rescaled probability of not switching $P_{\text{not}} = 1 - P(t)$ is fitted with a single exponential function.

Finally, we calculated the coercivity as a function of the temperature. The external field was applied at 0° with respect to the

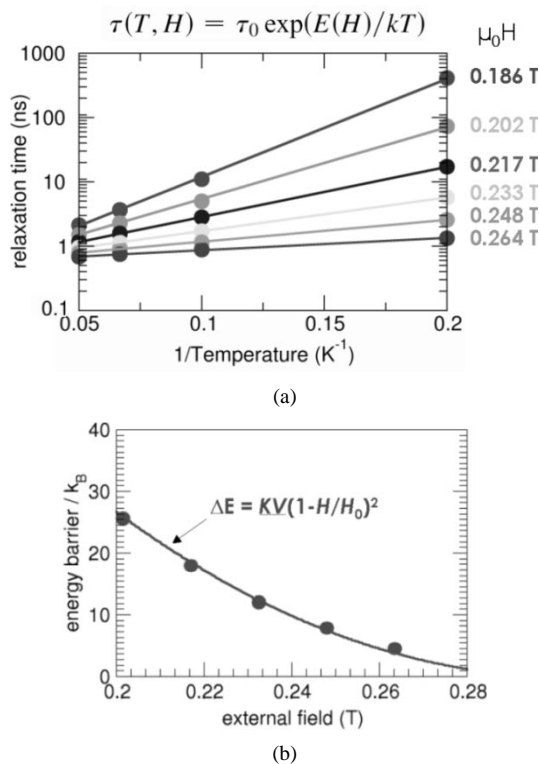


Fig. 2. (a) Relaxation time for spontaneous rotation of a small Co particle at nonzero temperature and zero applied field. (b) The derived energy barrier as a function of the applied field.

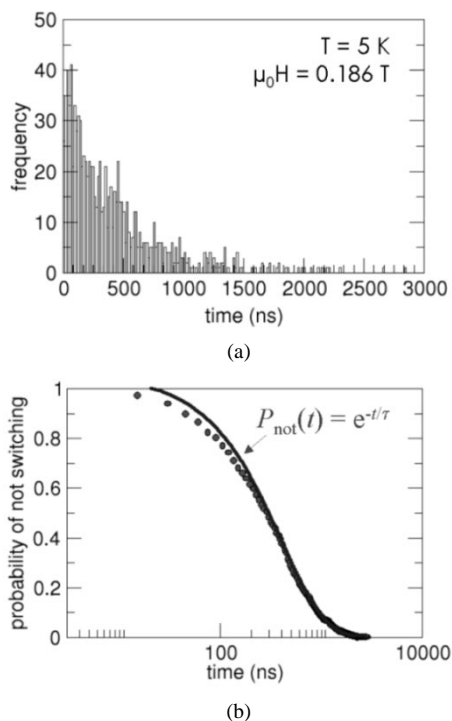


Fig. 3. (a) Waiting time histogram. (b) Probability of not switching.

z axis and at 45° with respect to the easy axis. Again, the numerical results were compared with experimental data and theoretical predictions [13]. The coercive field decays with $T^{1/2}$ and $T^{2/3}$ for an external field applied at 0° and 45° , respectively (see Fig. 4). The calculated coercive field is independent of the Gilbert damping constant.

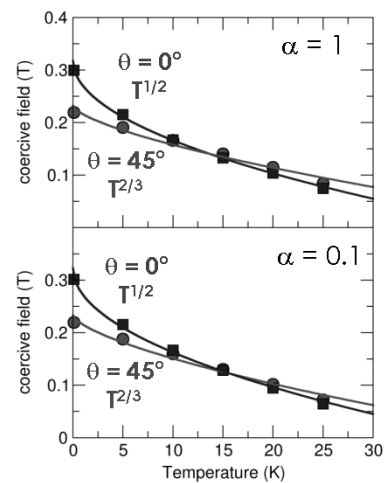


Fig. 4. Numerically calculated coercive field as a function of temperature of the Co nanoparticle. The external field was applied at zero and at 45° with respect to the easy axis. The Gilbert damping constant was $\alpha = 1$ (top) and $\alpha = 0.1$ (bottom).

V. CONCLUSION

Numerical experiments for thermally activated switching of small Co particles were performed solving the stochastic Gilbert equation. For low-energy barriers, the numerical results agree well with the Neel–Brown theory. Agreement with the theory was found for telegraph noise experiment, waiting time experiments, and the coercivity as a function of temperature. The numerically calculated attempt frequency was higher than measured experimentally.

REFERENCES

- [1] N. Smith and P. Arnett, "Thermal magnetization noise in spin valves," *IEEE Trans. Magn.*, vol. 38, pp. 32–37, 2002.
- [2] N. D. Rizzo, M. DeHerrera, J. Janesky, B. Engel, J. Slaughter, and S. Tehrani, "Thermally activated magnetization reversal in submicron magnetic tunnel junctions for magnetoresistive random access memory," *Appl. Phys. Lett.*, vol. 80, pp. 2335–2337, 2002.
- [3] D. Weller and A. Moser, "Thermal effect limits in ultrahigh-density magnetic recording," *IEEE Trans. Magn.*, vol. 35, pp. 4423–4439, Nov. 1999.
- [4] G. Brown, M. A. Novotny, and P. A. Rikvold, "Langevin simulation of thermally activated magnetization reversal in nanoscale pillars," *Phys. Rev. B*, vol. 64, p. 134422, 2001.
- [5] U. Nowak, "Thermally activated reversal in magnetic nanostructures," *Ann. Rev. Comp. Phys.*, vol. 9, p. 105, 2001.
- [6] W. F. Brown, "Thermal fluctuations of a single-domain particle," *Phys. Rev.*, vol. 130, pp. 1677–1686, 1963.
- [7] M. J. Werner, "Quantum statistics of fundamental and higher-order coherent quantum solitons in Raman-active waveguides," *Phys. Rev. A*, vol. 54, pp. R2567–R2570, 1996.
- [8] T. Schrefl, W. Scholz, D. Suess, and J. Fidler, "Langevin micromagnetics of recording media using subgrain discretization," *IEEE Trans. Magn.*, vol. 36, pp. 3189–3191, Sept. 2000.
- [9] W. F. Brown Jr., *Micromagnetics*. New York: Interscience, 1963.
- [10] M. J. Werner and P. D. Drummond, "Robust algorithms for solving stochastic partial differential equations," *J. Comp. Phys.*, vol. 132, pp. 312–326, 1997.
- [11] L. F. Shampine, *Numerical Solution of Ordinary Differential Equations*. New York: Chapman Hall, 1994.
- [12] "MATLAB User's Guide," The Mathworks, Inc., Natick, MA, 1993.
- [13] W. Wernsdorfer, "Classical and quantum magnetization reversal studied in nanometer-sized particles and clusters," in *Advances in Chemical Physics*, S. A. Rice, Ed. New York: Wiley, 2001.